RESEARCH ARTICLE

Synthesis and characterization of a non-planar cyclophenylene on Au(111)

Sergio Salaverria,[‡,[a]] Martin Irizar, [‡,[b],[c],[d]] Jesús Janeiro, [‡,[e]] Paula Angulo-Portugal,[[f]] Tao Wang,[[b],[g]] Jan Patrick Calupitan,[†,[f]] Jonathan Rodríguez-Fernández,[[a],[h]] Aran Garcia-Lekue,[[b],[i]] Martina Corso,[[f]] Emilio Artacho,[[b],[c],[i],[j]] Diego Peña,[[e]] Dolores Pérez,*[,[e]] and Dimas G. de Oteyza*[,[a],[b]]

[a] S. Salaverria, J. Rodríguez-Fernández, D. G. de Oteyza
Nanomaterials and Nanotechnology Research Center (CINN), CSIC-UNIOVI-PA
33940 El Entrego, Spain
E-mail: d.g.oteyza@cinn.es

[b] M. Irizar, T. Wang, A. García Lekue, E. Artacho, D. G. de Oteyza
Donostia International Physics Center
20018 San Sebastián, Spain
E-mail: d.g.oteyza@cinn.es

[c] M. Irizar, E. Artacho
CIC nanoGUNE-BRTA
20018 San Sebastián, Spain

[d] M. Irizar,
Department of Polymers and Advanced Materials: Physics, Chemistry and Technology, Faculty of Chemistry
University of the Basque Country UPV/EHU
20018 San Sebastián, Spain

[e] J. Janeiro, D. Peña, D. Pérez
Centro Singular de Investigación en Química Biolóxica e Materiais Moleculares (CiQUS) and Departamento de Química Orgánica, Universidade de Santiago de Compostela
15782 Santiago de Compostela, Spain
E-mail: dolores.perez@usc.es

[f] P. Angulo-Portugal, J. P. Calupitan, M. Corso
Centro de Física de Materiales (CFM-MPC), CSIC-UPV/EHU
20018 San Sebastián, Spain

[g] T. Wang
State Key Laboratory of Organometallic Chemistry, Shanghai Institute of Organic Chemistry, University of Chinese Academy of Sciences, Chinese Academy of Sciences
Shanghai 200032, China

[h] J. Rodríguez-Fernández
Physics Department,
University of Oviedo
33007 Oviedo, Spain

[i] A. Garcia-Lekue, E. Artacho
Ikerbasque, Basque Foundation for Science
48013 Bilbao, Spain

[j] E. Artacho
Theory of Condensed Matter, Cavendish Laboratory
University of Cambridge
Thomson Ave., Cambridge CB3 0HE, United Kingdom

[‡] These authors contributed equally

[†] Current address: Sorbonne Université, CNRS, Institut Parisien de Chimie Moléculaire, IPCM, F-75005 Paris, France

Supporting information for this article is given via a link at the end of the document.

Abstract: We report the surface-assisted synthesis of a non-planar cyclophenylene derivative containing four *meta*- and two *para*-connected phenylene moieties on Au(111), via hierarchical Ullmann coupling of a 1,10-dibrominated angular [3]phenylene and subsequent C–C bond cleavage at the four-membered rings. Scanning tunneling microscopy and spectroscopy (STM/STS) were used for the characterization of its chemical structure and electronic

properties. Density functional theory (DFT) calculations support the experimental observations.

Introduction

Cyclophenylenes, *i.e.*, macrocycles composed of linked benzene rings, have attracted intensive interest because of their appealing structures and potential applications[1] derived from their optoelectronic properties,[2–4] their rich size-dependent supramolecular chemistry[5] and their potential as platforms to build molecular nanobelts[6] or carbon nanotubes.[7,8] Several families of cyclophenylenes exist, classified according to the linking pattern of phenylene moieties, *i.e.*, connections *via* all *ortho*- (cyclo-*ortho*-phenylenes, [*n*]COPs), all *meta*- (cyclo-*meta*-phenylenes, [*n*]CMPs) or all *para*-substitution (cyclo-*para*-phenylenes, [*n*]CPPs), together with combinations of *meta*- (or *ortho*-) and *para*- connection patterns (Figure 1a). The synthesis of cyclophenylenes of all the aforementioned types has been achieved in solution-phase chemistry, from the early reports on the preparation of [*n*]COPs[9] and [*m*]CMPs,[10] or the challenging synthesis of [*n*]CPPs achieved years later by Bertozzi and Jasti,[11,12] to the plethora of recent examples of the construction of carbon nanohoops based on [*n*]CPPs[3] or on twisted derivatives incorporating *meta*- or *ortho*-phenylene linkages.[13–17]

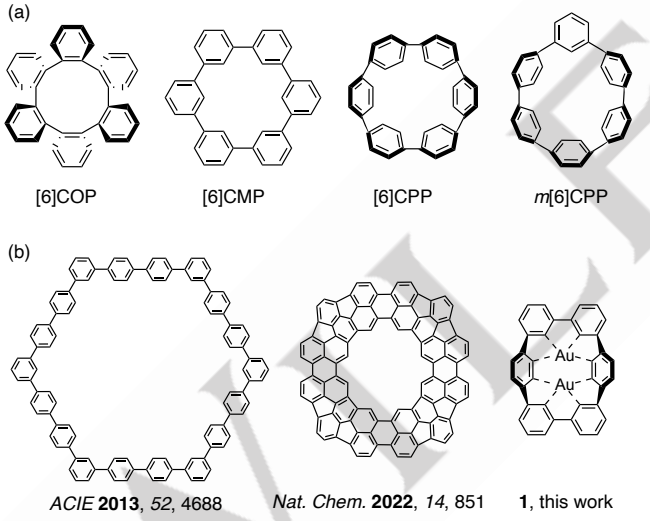

Figure 1. (a) Examples of cyclophenylenes with different connections between benzene rings, accessed by solution-phase synthesis. (b) Examples of cyclophenylenes and derivatives obtained by surface-assisted synthesis.

The recently developed field of on-surface synthesis (OSS) offers unprecedented opportunities for the fabrication of various novel cyclophenylenes with intriguing physical-chemical properties (Figure 1b).[18–23] The metal surface plays a vital role in facilitating reactions of synthetic interest, including bond-forming and bond-breaking reactions, as well as stabilizing species that would otherwise be unstable. In addition, OSS alleviates synthetic limitations by eliminating the need for solubility. The two-dimensional (2D) confinement of a solid surface also impacts the OSS reactions generally promoting planar product structures.[24,25]

To our knowledge, the few examples reported to date of cyclophenylenes obtained by OSS have a (*quasi*-) planar configuration, including two large CMPs[21,22] and a π-extended, planarized CPP derivative.[23] However, the synthesis of 3D cyclophenylenes (COPs, CPPs or *o*-/*m*-CPPs) has remained elusive on a 2D surface. It is worth to mention that both the currently reported OSS approaches and most of the solution-phase syntheses of cyclophenylenes, involve metal-catalyzed (or metal-assisted) coupling reactions between adequately functionalized arylene or polyarylene precursors, typically dihalogenated building blocks. Notably, the formation of [*n*]COPs (n = 4–10) by thermolysis of biphenylenes has been reported recently,[26] in a reaction that involves the homolytic ring-opening of the strained four-membered ring present in the biphenylene core.

In this work, we report the OSS of a non-planar Au-coordinated cyclophenylene **1** (Figure 1b), containing four *meta*- and two *para*-connections, on a Au(111) surface, by undergoing hierarchical, metal-assisted double Ullmann coupling of a 1,10-dibrominated angular [3]phenylene **2**, and subsequent selective C–C bond cleavage of the four-membered rings in the resulting [3]phenylene dimer. The chemical structure was characterized by bond-resolving (BR) STM and further supported by STS and DFT. This study offers the first approach for the synthesis of non-planar cyclophenylenes on surfaces.

Results and Discussion

The synthesis of the molecular precursor, a dibrominated angular [3]phenylene (1,10-dibromobenzo[3,4]cyclobuta[1,2-a]biphenylene, **2**) was achieved as shown in Scheme 1. A selective double Sonogashira coupling between trimethylsilylacetylene (TMSA) and 1,2-bis(2-bromo-6-iodophenyl)ethyne (**3**),[27] followed by mild desilylation of the resulting product gave triyne **4** in an excellent 95% overall yield. As the key step to build the angular [3]phenylene core, the intramolecular [2+2+2] cycloaddition catalyzed by CpCo(CO)(fum)[28] successfully afforded compound **2** in a 27% yield, a remarkable result considering that the reaction involves the construction of a highly strained polycyclic system.

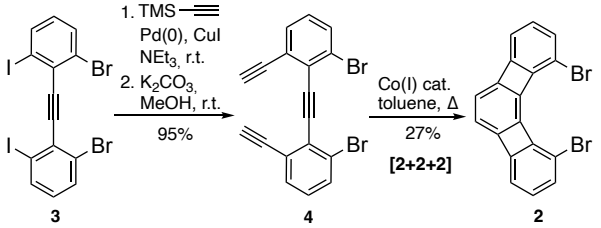

Scheme 1. Synthesis of angular 1,10-dibromo[3]phenylene **2**.

Deposition of **2** on a Au(111) surface held at RT under ultra-high vacuum (UHV) and subsequent annealing to 250 °C triggers the

heterolytic cleavage of the labile C−Br bonds. Then, the Br atoms remain adsorbed on the surface, whereas the organic sigma radicals are predominantly passivated by Au adatoms and only occasionally from covalent bonds with neighboring molecules to form S-shaped dimers (Fig. S1). Instead, by depositing **2** on a Au(111) surface held at 300 °C, alternative reaction pathways with higher activation barriers compete kinetically, allowing for the formation of additional products, as revealed in the STM image in Figure 2a (experiments at even higher temperature close to 400 °C simply prevented molecular adsorption and appeared as clean Au(111) surfaces). Most typical products are marked by different colored circles in Figure 2a and their corresponding BR-STM images are shown in Figs. 2b-e. The predominant product is a monomer with one or two sharp lines at the originally Br-functionalized atoms and a self-assembled dimer (>85%; Figs. 2b-c). The possibility that the sharp features belong to C−Br bonds can be excluded because the dissociation of phenyl-Br bonds on Au(111) typically completes around 150 °C.[29–31] Although the resulting Br adatoms adsorbed on Au(111) are not visible on the sample in Figure 2, they are clearly resolved on higher-coverage samples (Fig. S2). Therefore, the products are assigned to organometallic species generated from the coordination between Au adatom and debrominated monomer.[31,32] The organometallic bonds are resolved as a sharp lines in the BR-STM images (Figs. 2b-c) and Au adatoms appear as bright dots in a conventional STM image, in agreement with previous works.[31,32] For those originally Br-functionalized atoms that do not display coordinated Au adatoms, we can discard a bond to a Au surface atom, since that would distort the molecular planarity and the image contrast. We thus assume either a σ-radical that remains unpassivated in the inert UHV environment,[Pavlicek et al., ACS Nano 2017, 11, 10768−10773] a hydrogenation by the residual hydrogen pressure in presence of the ionizing filaments of the chamber's ion gauges,[Jimenez-Martín et al., ACS Nano 2024, 43, 29902–29912] or a mixture of the two cases.

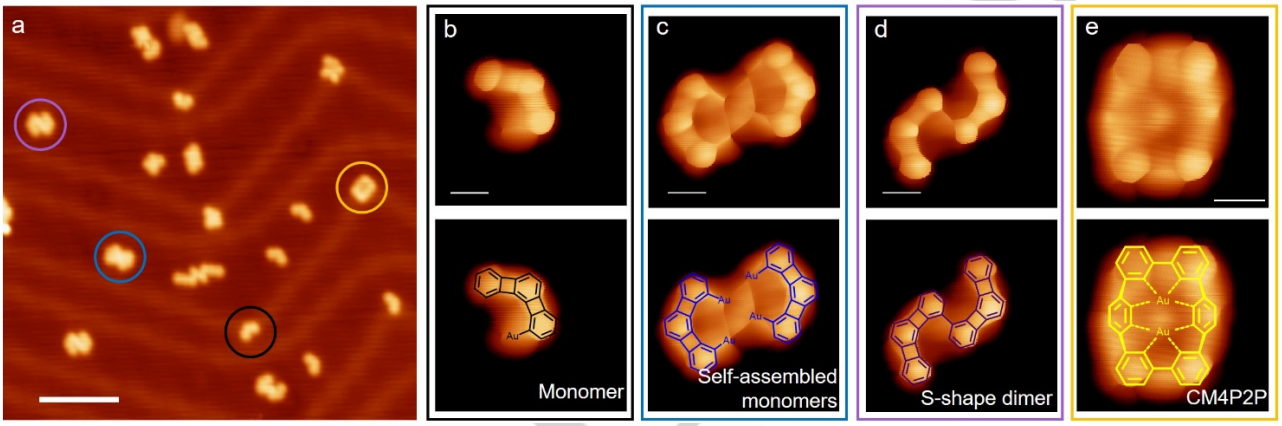

Figure 2. (a) Large STM image (-500 mV, 100 pA) of the sample prepared by depositing **2** on Au(111) held at 300 °C. Typical products are marked by different coloured circles. (b-e) Bond resolving STM images (constant height, 5 mV) of the different products marked in (a), obtained by CO functionalized tip, along with their corresponding chemical structures. Scale bar: (a) 5 nm, (b-e) 4 Å.

The two dominating products resulting from covalent C–C bond formation are displayed in Figures 2d-e. The S-shaped dimer (~10%; Figure 2d) is the most intuitive reaction product which can be obtained by metal-assisted Ullmann-type coupling and debromination of **2**. All four-membered rings stay intact in this product, as clearly resolved in the corresponding BR-STM images. A BR-STM image of the less intuitive covalent dimeric product (≈3%) is presented in Figure 2e, exhibiting a rectangular shape. Four *m*-phenylene moieties at the corners are nicely resolved, while other two are less clear due to their tilted configuration out of the surface (or molecular) plane.[33] The non-planarity implies that the four-membered rings have been cleaved on the Au(111) surface, similarly to the results reported in our previous work on Cu(111).[34] The product was assigned as the organometallic species **1**, a Au-coordinated cyclophenylene with two *para*- and four *meta*- linkages between adjacent benzene rings. The proposed structure is strongly supported by the match between the BR-STM image and the chemical structure of **1** (Figure 2e), as well as by DFT calculations (see below).

We also study the electronic properties of **1** by means of scanning tunneling spectroscopy (STS). Figure 3a presents the dI/dV spectra obtained on top of the molecule. A well-defined resonance is resolved for the highest occupied molecular orbital (HOMO) at -1.3 eV. Within the probed energy range we only observe a clearly rising intensity from 1.2 eV onwards for the unoccupied states. Although the precise energy of the lowest unoccupied molecular orbital (LUMO) is therefore uncertain, we can infer a relatively large HOMO-LUMO gap ≥ 2.5 eV. Conductance maps acquired on the low energy tail of the HOMO (-1.2 eV) and around the onset of the rising intensity of unoccupied states (1.3 eV) are shown in Figure 3b and Figure 3c, respectively, and their good match to the calculated STM images for the HOMO and LUMO further support the structural assignment. It should be noted that alternative structures with and without additional hydrogenation (Figures S5 and S6) have also been calculated and were discarded due to misfit of experiment and theory.

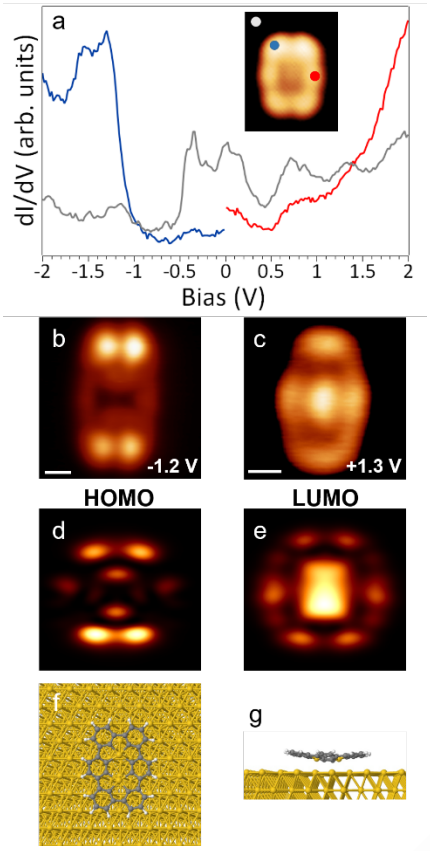

Figure 3. (a) dI/dV point spectra on **1** on the Au(111) substrate, acquired at the positions marked in the inset with the correspondingly colored points (gray thus corresponds to the reference spectrum on Au). Dashed lines mark the energies of the conductance maps shown below. (b-c) Experimental conductance maps at -1.2 eV 1.3 eV, respectively. (d-e) STM simulations of the HOMO and LUMO of the molecule on Au(111), respectively. (f) Top and (g) side-views of the relaxed molecular structure adsorbed on Au(111)Scale bar: (b-e) 4 Å.

The relatively large HOMO-LUMO gap of **1**, which is predicted to be $E_g \approx 2.2$ eV by DFT, is due to the weak π-conjugation between the six phenylenes. In the first place, the quantum interference or cross-conjugation of the *meta*-connections divides the molecule into four potentially conjugated segments[35–37] of three and two phenylene units. However, the tilted configuration of the two central phenyl rings along the terphenylene sides again breaks the associated π-conjugation.[33,38] In contrast, the phenylene coplanarity on the short sides renders these the largest conjugated segments, which consequently host most of the frontier orbital electron density.

The proposed reaction mechanism behind the formation of **1** is as shown in Scheme 2. After debromination of **2**, not only one single Ullmann-type coupling forming the S-shaped covalent [3]phenylene dimer **6** is activated, but also the double coupling can occur, generating a highly strained macrocyclic [3]phenylene dimer **7** with four-membered cyclobutadiene rings. Because of the high strain of this non-detected, intermediate product, it becomes favorable the opening of the four-membered rings by selective, metal-assisted C–C bond activation,[34] leading to the formation of the final organometallic product **1**. The radicals presumably generated from the cleavage of four-membered rings coordinate with Au adatoms, which appear as a central dot in the BR-STM image in Figure 2e. It is worth to note that the observed fourfold C–C bond activation occurs with the same regioselectivity as that reported for the metal-catalyzed reactions of [3]phenylene in solution, involving the metal insertion into the C–C bonds at the inner-rim of the angular [3]phenylene system.[39–41]

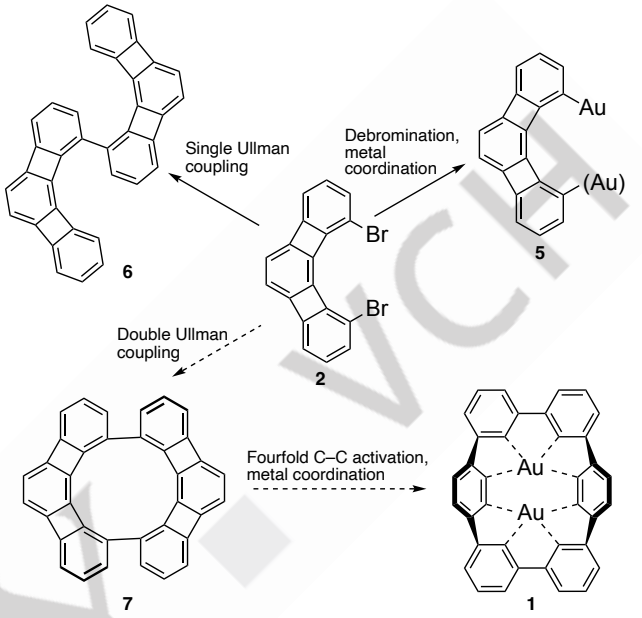

Scheme 2. Reaction of precursor **2** on Au(111), *via* metal coordination and Ullmann-coupling, along with the chemical structures of the products and of intermediate [3]phenylene dimer **7**.

The formation of a non-planar product *via* Ullmann coupling of planar reactants, as occurs in the initial reaction from **2** to **7**, is unconventional on a 2D metal surface. Here we note that the order in which the reactions occur plays a decisive role in the reaction producing **1** on Au(111), *i.e.*, Ullmann coupling occurs before the bond cleavage of a four-membered ring. In fact, it is the strain in **7** which facilitates the fourfold C–C bond activation. Besides, otherwise terphenyls holding multiple radicals would be generated from the cleavage of four-membered rings, which would then easily couple into rhombus-shaped nanographenes. Although such rhombus products were occasionally observed in our experiment (Figure S3), it is not possible to create **1** from this rhombus-shaped product due to the thermodynamic stability of such fully-benzenoid carbon nanostructure.[34]

The proposed Au-coordinated cyclophenylene derivative **1** is thermodynamically relatively stable and according to our experiments it remains intact even when annealing the sample to >400 °C (Figure S4). This was further confirmed by gas-phase DFT calculations, where the coordination to two gold atoms is a necessary condition to stabilize the structure resulting from the fourfold C–C bond breakage, with four *meta*- and two *para*-linked phenylenyl radicals. In the absence of such gold atoms, neighboring *meta*-phenylenyl radicals tend to form four-membered rings whereas in the presence of a single gold atom it cannot be stabilized without a loss of symmetry in the structural

and electronic properties (see SI Figure S5). Furthermore, the DFT results for the molecule adsorbed on Au(111) endorse the idea that the molecular stabilization is mediated preferably by the incorporation of two gold adatoms, but in their absence, the molecule is avid enough to pull them out of the clean surface (see SI Figure S7).

Conclusion

In conclusion, starting from the 1,10-dibrominated angular [3]phenylene **2**, we successfully synthesized a Au-coordinated non-planar cyclophenylene, *via* dimerization through a double Ullmann coupling followed by a fourfold regioselective C–C σ-bond activation at the four-membered rings of the dimeric macrocycle. STS and DFT calculations reveal that **1** has a relatively large energy gap owing to the weak π electron conjugation as disrupted by tilting side/lateral phenylenes. Our study provides new perspectives for the synthesis of 3D cyclophenylenes and other carbon frameworks on solid surfaces.

Experimental Section

General synthetic methods: All reactions were carried out under argon using oven-dried glassware. Toluene was taken from a MBraun SPS-800 Solvent Purification System. Et3N was dried over CaH2. Other commercial reagents were purchased from ABCR GmbH, Sigma-Aldrich or Acros Organics, and were used without further purification. Deuterated solvents were purchased from Acros Organics. Thin layer chromatography was performed on Merck silica gel 60 F254 and chromatograms were visualized with UV light (254 and 365 nm) and/or stained with Hanessian's stain. Column chromatography was performed on Merck silica gel 60 (ASTM 230-400 mesh). ^{1}H and ^{13}C-NMR spectra were recorded at 300 and 75 MHz (Varian Mercury-300 instrument), 500 and 125 MHz (Varian Inova 500 or Bruker 500) or 750 MHz (Bruker NEO 750 instrument) respectively. Low-resolution mass spectra (EI) were obtained at 70 eV on a HP5988A instrument, while high-resolution mass spectra (HRMS) were obtained on a Micromass Autospec spectrometer. APCI high resolution mass spectra were obtained on a Bruker Microtof instrument.

Synthesis of 1,2-bis(2-bromo-6-ethynylphenyl)ethyne (4): (1) To a degassed solution of 1,2-bis(2-bromo-6-iodophenyl)ethyne (**3**)[27] (1.5 g, 2.55 mmol), $PdCl_2(PPh_3)_2$ (0.179 g. 0.255 mmol), CuI (0.097g, 0.510 mmol) in dry Et_3N (335 mL), trimethylsilylacetylene (4.2 mL, 29.67 mmol) was added. The mixture was stirred for 16h at room temperature. After that, the solvent was removed under reduced pressure and the crude material was purified by column chromatography (SiO_2, hexane) isolating 1,2-bis[2-bromo-6-((trimethylsilyl)ethynyl)phenyl]ethyne as a yellow oil (1.290 g, 96%). ^{1}H NMR (500 MHz, $CDCl_3$), δ: 7.57 (dd, *J* = 8.1, 1.2 Hz, 2H), 7.46 (dd, *J* = 7.8, 1.2 Hz, 2H), 7.11 (t, *J* = 7.9 Hz, 2H), 0.18 (s, 18H). ^{13}C NMR-DEPT (75 MHz, $CDCl_3$), δ: 132.49 (2xCH), 131.38 (2xCH), 129.04 (2xCH), 128.11 (2xC), 127.83 (2xC), 125.74 (2xC), 102.86 (2xC), 100.58 (2xC), 94.98 (2xC), 0.01 ($3xCH_3$). HRMS(APCI-FIA-TOF) for $C_{24}H_{24}Br_2Si_2$ ([M]$^+$) Calcd.: 525.9778; Found: 525.9779. (2) To a solution of the previously prepared bis(trimethylsilyl)ethynyl derivative (1.290 g, 2.441 mmol) in MeOH (13 mL), K_2CO_3 (1.619 g, 11.78 mmol) was added. The mixture was reacted until starting material was consumed (TLC, 3 h). Then, the reaction was stopped by adding water. The aqueous layer was extracted with ethyl acetate and the combined organic layers were washed with ammonium chloride 5% solution twice and dried over sodium sulfate affording **4** as a brown solid (0.925 g, 99%) which was used in the next step without any further purification. ^{1}H-NMR (500 MHz, $CDCl_3$), δ: 7.62 (dd, *J* = 8.2, 1.2 Hz, 2H), 7.49 (dd, *J* = 7.8, 1.2 Hz, 2H), 7.15 (t, *J* = 7.9 Hz, 2H), 3.36 (s, 2H). ^{13}C-NMR-DEPT (75 MHz, $CDCl_3$), δ: 133.32 (2xCH), 131.99 (2xCH), 129.47 (2xCH), 128.17 (2xC), 127.26(2xC), 126.48 (2xC), 94.88 (2xC), 83.20 (2xCH), 82.03(2xC). HRMS (APCI-DIP-TOF) for $C_{18}H_{18}Br_2$ ([M]$^+$) Calcd.: 381.8987; Found: 381.8974.

Synthesis of 1,10-dibromobenzo[3,4]cyclobuta[1,2-*a*]biphenylene (2): Compound **4** (100 mg, 0.260 mmol) and CpCo(CO)(fum) (77.4 mg, 0.260 mmol) were placed in a dry 100 mL round bottom flask under Ar atmosphere. Then, dry toluene was added (52 mL) and the mixture was thoroughly degassed and refluxed for 3h. After that, volatiles were removed under reduced pressure and the crude material was purified by column chromatography (SiO_2, Hexane/DCM; 9:1) yielding **2** as a yellow solid (27mg, 27%). ^{1}H-NMR (300 MHz, $CDCl_3$), δ: 7.05 (d, *J* = 8.4 Hz, 2H), 6.85 (dd, *J* = 8.4, 6.9 Hz, 2H), 6.79 (d, *J* = 6.9 Hz, 2H), 6.21 (s, 2H). ^{13}C-NMR-DEPT (75 MHz, $CDCl_3$), δ: 152.08 (2xC), 149.05 (2xC), 148.04 (2xC), 135.19 (2xC), 132.48 (2xCH), 131.00 (2xCH), 116.93 (2xCH), 115.20 (2xCH), 112.85 (2xC). HRMS (APCI-DIP-TOF) for $C_{18}H_{18}Br_2$ ([M]$^+$) Calcd.: 381.8987; Found: 381.8989.

STM experiments: STM measurements were performed using a commercial Scienta-Omicron LT-STM at 77.4 K and 4.3 K. The system consists of a preparation chamber with a typical pressure in the low 10^{-10} mbar regime and a STM chamber with a pressure in the 10^{-11} mbar range. The Au(111) crystal was cleaned via two cycles of Ar^+ sputtering and annealing at 720 K. The precursor molecule **2** was evaporated from a home-built molecular evaporator at 383 K. The efficient molecular flux is approximately 0.1 monolayer per minute on the Au(111) surface. All STM and STS measurements were performed at 77.4 K, except the BR-STM images, which were measured at 4.3 K. To obtain BR-STM images, the tip was functionalized with a CO molecule that was picked up from the Au(111) surface. CO was dosed into the STM chamber via a leak valve at a pressure of approximately 1×10^{-8} mbar. For adsorption onto the sample, the STM thermal shields were opened and closed again when reaching a sample temperature of 7.0 K. Three such shield opening cycles were typically applied. CO can be picked up with a metallic tip by scanning with a high current and negative bias (e.g. I = 1 nA, U = −0.5 V). dI/dV measurements were recorded with the internal lock-in of the Nanonis electronics. The oscillation frequency used in experiments is 731 Hz and the amplitude is 20 mV for all STS and dI/dV maps shown in the manuscript .

Computational Methods

First principles calculations were performed via Density Functional Theory (DFT) as implemented in the SIESTA package.[43-45] Dispersive interactions were considered via the van der Waals (vdW) density functional by Dion *et al.*,[46] reparametrized by Klimeš, Bowler and Michaelides.[47] The Au(111) surface was constructed by a 4-layer slab, where we adopted an extended double-zeta-polarised (DZP) basis optimized for the Au(111) surface description.[48] The remaining basis set was described by a 100 meV energy shift along with a split norm of 0.15. We used a 17.3 x 24.98 Å^2 slab (6 x 5 supercell) for a molecule of size 8.2 x 11.2 Å^2 and a cell parameter of 20 Å in the direction perpendicular to the surface to avoid the effects of the interaction between molecules in neighboring cells. The supercell laterally corresponds to a lattice parameter of a= 4.07 Å, which is the theoretical value obtained from a bulk relaxation using the same technical details presented here. Due to the dimension of the supercell, we found that our calculations are converged if a Γ only k-point sampling is employed. Moreover, the bottom Au surface was passivated with hydrogen atoms to quench its Au(111) surface state (SS), avoiding spurious effects due to the interaction of the surface states on both sides of the slab.[49] These hydrogens are placed following the ABC stacking of Au(111) at a relaxed distance of 1.13 Å from the closest Au plane. The core electrons have been described by the norm-conserving Troullier-Martins pseudopotentials[50] and generated with the ATOM package included in the SIESTA software, the cutoff radii being (all in bohr units) 1.54 for the s, p, d, and f channels of C; 2.60 , 2.77 , 2.60 and 2.60 for bulk Au; 2.50, 2.70, 2.50 and 2.50 for surface Au and 1.25 for H. The molecule and the first 2 gold layers were allowed to relax up to a force tolerance of 40 meV/Å and the rest of the slab has its atoms at the bulk positions according to the same calculated lattice parameter a=4.07 Å.

Scanning Tunneling Microscopy (STM) simulations were performed using a SIESTA utility, called STM, which is based on the Tersoff-Hamman approximation.[51]

Supporting Information

Further experimental and computational details are given in the Supporting Information file.

Acknowledgements

This work was supported by grants PID2022-140845OB-C62, PID2022-140845OB-C64, PID2022-140845OB-C66 and PID2022-139933NB-I00, funded by the Spanish MCIN/AEI/ 10.13039/501100011033 and FEDER Una manera de hacer Europa. We also acknowledge grants TED2021-132388B-C43 and TED2021-132388B-C44, funded by the Spanish MCIN/AEI/ 10.13039/501100011033 and the European Union "NextGenerationEU"/PRTR. Further support is acknowledged from the European Union Horizon 2020 through FET-Open Project SPRING (Grant No. 863098) and ERC Synergy Grant MolDAM (951519), the Xunta de Galicia (Centro de investigación do Sistema universitario de Galicia accreditation 2023-2027, ED431G 2023/03) and the European Union (European Regional Development Fund - ERDF). A.G-L also acknowledges the financial support received from the IKUR Strategy under the collaboration agreement between Ikerbasque Foundation and DIPC on behalf of the Department of Education of the Basque Government. E.A. further acknowledges a María de Maeztu award to Nanogune, Grant No. CEX2020-001038-M, funded by MCIN/AEI/10.13039/501100011033, and the Quantum Sense project of the Diputación General de Gipuzkoa. JJ thanks the AEI for the award of a pre-doctoral fellowship (PRE2020-092897).

Keywords: Cyclophenylene • on-surface synthesis • metal-coordination • scanning tunneling microscopy • density functional theory

[1] E. J. Leonhardt, R. Jasti, *Nat. Rev. Chem.* **2019**, *3*, 672–686.
[2] M. R. Golder, R. Jasti, *Acc. Chem. Res.* **2015**, *48*, 557–566.
[3] S. E. Lewis, *Chem. Soc. Rev.* **2015**, *44*, 2221–2304.
[4] F. Lucas, C. Brouillac, N. McIntosh, S. Giannini, J. Rault-Berthelot, C. Lebreton, D. Beljonne, J. Cornil, E. Jacques, C. Quinton, C. Poriel, *Chemistry A European J* **2023**, *29*, e202300934.
[5] Y. Xu, M. Von Delius, *Angew. Chem. Int. Ed.* **2020**, *59*, 559–573.
[6] K. Y. Cheung, S. Gui, C. Deng, H. Liang, Z. Xia, Z. Liu, L. Chi, Q. Miao, *Chem* **2019**, *5*, 838–847.
[7] Q. Huang, G. Zhuang, M. Zhang, J. Wang, S. Wang, Y. Wu, S. Yang, P. Du, *J. Am. Chem. Soc.* **2019**, *141*, 18938–18943.
[8] S. Wang, F. Chen, G. Zhuang, K. Wei, T. Chen, X. Zhang, C. Chen, P. Du, *Nano Res.* **2023**, *16*, 10342–10347.
[9] G. Wittig, G. Lehmann, *Chem. Ber.* **1957**, *90*, 875–892.
[10] H. A. Staab, F. Binnig, *Tetrahedron Letters* **1964**, *5*, 319–321.
[11] R. Jasti, J. Bhattacharjee, J. B. Neaton, C. R. Bertozzi, *J. Am. Chem. Soc.* **2008**, *130*, 17646–17647.
[12] J. Xia, R. Jasti, *Angew. Chem. Int. Ed.* **2012**, *51*, 2474–2476.
[13] T. C. Lovell, C. E. Colwell, L. N. Zakharov, R. Jasti, *Chem. Sci.* **2019**, *10*, 3786–3790.
[14] A. Bu, Y. Zhao, H. Xiao, C. Tung, L. Wu, H. Cong, *Angew. Chem. Int. Ed.* **2022**, *61*, e202209449.
[15] X.-W. Chen, K.-S. Chu, R.-J. Wei, Z.-L. Qiu, C. Tang, Y.-Z. Tan, *Chem. Sci.* **2022**, *13*, 1636–1640.
[16] T. Terabayashi, E. Kayahara, Y. Zhang, Y. Mizuhata, N. Tokitoh, T. Nishinaga, T. Kato, S. Yamago, *Angew. Chem. Int. Ed.* **2023**, *62*, e202214960.
[17] R. Lingas, N. D. Charistos, A. Muñoz-Castro, *ChemPhysChem* **2021**, *22*, 741–751.
[18] S. Clair, D. G. de Oteyza, *Chem. Rev.* **2019**, *119*, 4717–4776.
[19] T. Wang, J. Zhu, *Surf. Sci. Rep.* **2019**, *74*, 97–140.
[20] Q. Fan, J. M. Gottfried, J. Zhu, *Acc. Chem. Res.* **2015**, *48*, 2484–2494.
[21] M. Chen, J. Shang, Y. Wang, K. Wu, J. Kuttner, G. Hilt, W. Hieringer, J. M. Gottfried, *ACS Nano* **2017**, *11*, 134–143.
[22] Q. Fan, C. Wang, Y. Han, J. Zhu, W. Hieringer, J. Kuttner, G. Hilt, J. M. Gottfried, *Angew. Chem. Int. Ed.* **2013**, *52*, 4668–4672.
[23] F. Xiang, S. Maisel, S. Beniwal, V. Akhmetov, C. Ruppenstein, M. Devarajulu, A. Dörr, O. Papaianina, A. Görling, K. Y. Amsharov, S. Maier, *Nat. Chem.* **2022**, *14*, 871–876.
[24] T. Wang, J. Lawrence, N. Sumi, R. Robles, J. Castro-Esteban, D. Rey, M. S. G. Mohammed, A. Berdonces-Layunta, N. Lorente, D. Pérez, D. Peña, M. Corso, D. G. De Oteyza, *Phys. Chem. Chem. Phys.* **2021**, *23*, 10845–10851.
[25] T. G. Lohr, J. I. Urgel, K. Eimre, J. Liu, M. Di Giovannantonio, S. Mishra, R. Berger, P. Ruffieux, C. A. Pignedoli, R. Fasel, X. Feng, *J. Am. Chem. Soc.* **2020**, *142*, 13565–13572.
[26] D. Ehjeij, F. Rominger, U. H. F. Bunz, J. Freudenberg, K. Müllen, *Angew. Chem. Int. Ed.* **2024**, *63*, e202312040.
[27] O. Š. Miljanić, S. HanPresent Address: Arena Pharmaceu, D. Holmes, G. R. Schaller, K. P. C. Vollhardt, *Chem. Commun.* **2005**, 2606.
[28] A. Geny, N. Agenet, L. Iannazzo, M. Malacria, C. Aubert, V. Gandon, *Angew. Chem. Int. Ed.* **2009**, *48*, 1810–1813.
[29] M. Fritton, D. A. Duncan, P. S. Deimel, A. Rastgoo-Lahrood, F. Allegretti, J. V. Barth, W. M. Heckl, J. Björk, M. Lackinger, *J. Am. Chem. Soc.* **2019**, *141*, 4824–4832.
[30] A. Batra, D. Cvetko, G. Kladnik, O. Adak, C. Cardoso, A. Ferretti, D. Prezzi, E. Molinari, A. Morgante, L. Venkataraman, *Chem. Sci.* **2014**, *5*, 4419–4423.
[31] A. Berdonces-Layunta, F. Schulz, F. Aguilar-Galindo, J. Lawrence, M. S. G. Mohammed, M. Muntwiler, J. Lobo-Checa, P. Liljeroth, D. G. de Oteyza, *ACS Nano* **2021**, *15*, 16552–16561.
[32] H. Zhang, J. Franke, D. Zhong, Y. Li, A. Timmer, O. D. Arado, H. Mönig, H. Wang, L. Chi, Z. Wang, K. Müllen, H. Fuchs, *Small* **2014**, *10*, 1361–1368.
[33] C. Moreno, X. Diaz De Cerio, M. Vilas-Varela, M. Tenorio, A. Sarasola, M. Brandbyge, D. Peña, A. Garcia-Lekue, A. Mugarza, *J. Am. Chem. Soc.* **2023**, *145*, 8988–8995.
[34] J. P. Calupitan, T. Wang, A. Pérez Paz, B. Álvarez, A. Berdonces-Layunta, P. Angulo-Portugal, R. Castrillo-Bodero, F. Schiller, D. Peña, M. Corso, D. Pérez, D. G. de Oteyza, *J. Phys. Chem. Lett.* **2023**, 947–953.
[35] I. Piquero-Zulaica, A. Garcia-Lekue, L. Colazzo, C. K. Krug, M. S. G. Mohammed, Z. M. Abd El-Fattah, J. M. Gottfried, D. G. de Oteyza, J. E. Ortega, J. Lobo-Checa, *ACS Nano* **2018**, *12*, 10537–10544.
[36] G. Calogero, I. Alcón, N. Papior, A.-P. Jauho, M. Brandbyge, *J. Am. Chem. Soc.* **2019**, *141*, 13081–13088.
[37] J. Lawrence, M. S. G. Mohammed, D. Rey, F. Aguilar-Galindo, A. Berdonces-Layunta, D. Peña, D. G. de Oteyza, *ACS Nano* **2021**, *15*, 4937–4946.
[38] M. S. Miao, P. E. Van Camp, V. E. Van Doren, J. J. Ladik, J. W. Mintmire, *J. Chem. Phys.***1998**, *109*, 9623–9631.
[39] S. Kumaraswamy, S. S. Jalisatgi, A. J. Matzger, O. Š. Miljanić, K. P. C. Vollhardt, *Angew. Chem. Int. Ed.* **2004**, *43*, 3711–3715.
[40] Z. Gu, G. B. Boursalian, V. Gandon, R. Padilla, H. Shen, T. V. Timofeeva, P. Tongwa, K. P. C. Vollhardt, A. A. Yakovenko, *Angew. Chem. Int. Ed.* **2011**, *50*, 9413–9417.
[41] A. Korotvička, I. Císařová, J. Roithová, M. Kotora, *Chem. Eur. J.* **2012**, *18*, 4200–4207.
[42] L. Feng, T. Wang, H. Jia, J. Huang, D. Han, W. Zhang, H. Ding, Q. Xu, P. Du, J. Zhu, *Chem. Commun.* **2020**, *56*, 4890–4893.
[43] E. Artacho, D. Sánchez-Portal, P. Ordejón, A. García, J. M. Soler, *Phys. Stat. Sol. (b)* **1999**, *215*, 809–817.

[44] J. M. Soler, E. Artacho, J. D. Gale, A. García, J. Junquera, P. Ordejón, D. Sánchez-Portal, *J. Phys.: Condens. Matter* **2002**, *14*, 2745–2779.

[45] A. García, N. Papior, A. Akhtar, E. Artacho, V. Blum, E. Bosoni, P. Brandimarte, M. Brandbyge, J. I. Cerdá, F. Corsetti, R. Cuadrado, V. Dikan, J. Ferrer, J. Gale, P. García-Fernández, V. M. García-Suárez, S. García, G. Huhs, S. Illera, R. Korytár, P. Koval, I. Lebedeva, L. Lin, P. López-Tarifa, S. G. Mayo, S. Mohr, P. Ordejón, A. Postnikov, Y. Pouillon, M. Pruneda, R. Robles, D. Sánchez-Portal, J. M. Soler, R. Ullah, V. W. Yu, J. Junquera, *J. Chem. Phys.* **2020**, *152*, 204108.

[46] M. Dion, H. Rydberg, E. Schröder, D. C. Langreth, B. I. Lundqvist, *Phys. Rev. Lett.* **2004**, *92*, 246401.

[47] J. Klimeš, D. R. Bowler, A. Michaelides, *J. Phys.: Condens. Matter* **2010**, *22*, 022201.

[48] S. García-Gil, A. García, N. Lorente, P. Ordejón, *Phys. Rev. B* **2009**, *79*, 075441.

[49] N. Gonzalez-Lakunza, I. Fernández-Torrente, K. J. Franke, N. Lorente, A. Arnau, J. I. Pascual, *Phys. Rev. Lett.* **2008**, *100*, 156805.

[50] N. Troullier, J. L. Martins, *Phys. Rev. B* **1991**, *43*, 1993–2006.

[51] J. Tersoff, D. R. Hamann, *Phys. Rev. B* **1985**, *31*, 805–813.

Entry for the Table of Contents

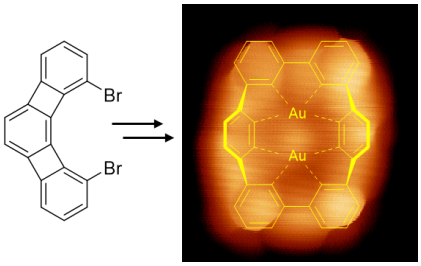

The construction of an unprecedent gold-complexed cyclophenylene with *meta*- and *para*-phenylene linkages has been achieved by means of on-surface promoted dimerization of a 1,10-dibrominated angular [3]phenylene followed by regioselective fourfold C–C σ-bond activation at the four-membered rings. This finding highlights the non-trivial on-surface reactivity of [*N*]phenylenes and opens new perspectives for the synthesis of 3D cyclophenylenes and other carbon frameworks on solid surfaces.

Institute and/or researcher Twitter usernames: @DoloresPMeiras, @dgoteyza, @ciqususc, @NanoCINN, @SPM_SumoLab